



National  
Defence

Défense  
nationale



AD-A247 667  
|||||

# THE TEMPERATURE DEPENDENCE OF A LARGE DYNAMIC RANGE PHOTODETECTOR STRUCTURE (U)

by

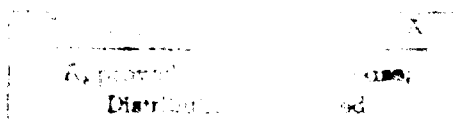
Robert J. Inkol

92 3 20 100

**DEFENCE RESEARCH ESTABLISHMENT OTTAWA**  
TECHNICAL NOTE 91-35

Canada

December 1991  
Ottawa



92-07135  
10115-10000



National  
Defence

Défense  
nationale



Accession For	
NTIS GRA&I	<input checked="checked" type="checkbox"/>
DTIC TAB	<input type="checkbox"/>
Unannounced	<input type="checkbox"/>
Justification	
By	
Distribution/	
Availability Codes	
Dist	Avail and/or Special
A-1	

# THE TEMPERATURE DEPENDENCE OF A LARGE DYNAMIC RANGE PHOTODETECTOR STRUCTURE (U)

by

**Robert J. Inkol**  
*Radar ESM Section*  
*Electronic Warfare Division*

**DEFENCE RESEARCH ESTABLISHMENT OTTAWA**  
TECHNICAL NOTE 91-35

PCN  
011LB

December 1991  
Ottawa

## ABSTRACT

A recently developed photodetector circuit exploits the exponential voltage-to-current characteristic of a MOSFET operated in the subthreshold region to achieve a logarithmic steady state response. This paper analyzes the temperature dependence of the circuit operation and presents experimental results demonstrating the capabilities and limitations of the model.

## RESUME

La réponse logarithmique en régime permanent d'un nouveau circuit pour photodétecteur est obtenue grâce à la relation exponentielle entre la tension et le courant d'un MOSFET opérant sous le seuil. Cette publication contient une analyse de l'opération du circuit en fonction de la température. Des résultats expérimentaux démontrent les capacités et les limitations du modèle présenté.

## EXECUTIVE SUMMARY

A recently developed photodetector circuit exploits the exponential voltage-to-current characteristic of a MOSFET operated in the subthreshold region to achieve a logarithmic steady state response. This paper analyzes the temperature dependence of the circuit operation and presents experimental data which is generally consistent with the model. It is observed that the behaviour of the photodetector is similar in some respects to that of a photodiode operated in the solar cell mode, but has a greater sensitivity to fabrication process parameters. A test circuit which would facilitate accurate measurements at low illumination levels is proposed.

# TABLE OF CONTENTS

	<u>PAGE</u>
ABSTRACT/RESUME	iii
EXECUTIVE SUMMARY	v
TABLE OF CONTENTS	vii
LIST OF FIGURES	ix
1.0 INTRODUCTION	1
2.0 CIRCUIT MODEL	1
2.1 MOSFET Model	1
2.2 Photodiode Model	6
3.0 ANALYSIS OF CIRCUIT MODEL FOR TEMPERATURE DEPENDENCE	7
4.0 EXPERIMENTAL RESULTS	9
5.0 DISCUSSION	12
6.0 REFERENCES	15
APPENDIX 1: IMPROVED TEST CIRCUIT FOR DC CHARACTERIZATION OF THE DYNAMIC RANGE PHOTODETECTOR CIRCUIT	A-1

## LIST OF FIGURES

	<u>PAGE</u>
FIGURE 1: LARGE DYNAMIC RANGE PHOTODETECTOR CIRCUIT	2
FIGURE 2: EXPERIMENT SET-UP	10
FIGURE 3: $V_{BS}$ (VOLTS) VS LIGHT ILLUMINATION ATTENUATION (INCREMENTS OF 0.3 dB/UNIT)	11
FIGURE A1: IMPROVED PHOTODETECTOR TEST CIRCUIT FOR DC CHARACTERIZATION	A-2

## 1.0 INTRODUCTION

The dynamic range of photodetectors is important in many applications. One solution is to operate a photodiode in the solar cell mode. The steady state open circuit output voltage is given by

$$V = \frac{mkT}{q} \ln \left( \frac{I_p + I_o}{I_o} \right) \quad (1)$$

where  $m$  is a constant between 1 and 2,  $k$  is Boltzmann's constant,  $T$  is the absolute temperature in degrees Kelvin,  $q$  is the charge of an electron,  $I_o$  is the reverse saturation current of the photodiode and  $I_p$  is the photocurrent. Since the photocurrent is proportional to the intensity of the illumination, the steady state response is logarithmic for  $I_p \gg I_o$ . Unfortunately, operation of photodiodes in the solar cell mode on a monolithic array requires dielectric isolation techniques to electrically isolate the photodiodes.

The recently developed photodetector circuit illustrated in Figure 1 uses the exponential voltage to current characteristic of a MOSFET operated in the subthreshold region to achieve a similar behaviour [1]. It is attractive for the implementation of monolithic arrays since it is compatible with standard MOS processing technology.

The temperature dependence of the circuit operation has not been considered in published analysis, but is potentially important in some applications. This is discussed in this report.

## 2.0 CIRCUIT MODEL

For unloaded steady state operation, the MOSFET source and photodiode currents,  $I_s$  and  $I_D$  respectively, satisfy the equality

$$I_s = I_D \quad (2)$$

With appropriate analytic behavioral models for  $I_D$  and  $I_s$ , this relationship can be evaluated to determine the circuit behaviour as a function of environmental and circuit parameters.

### 2.1 MOSFET Model

The behaviour of MOSFETs in the subthreshold region is of considerable significance in a number of applications. MOSFETs may be operated in the subthreshold region in low power analog circuits where the relatively high ratio of transconductance to

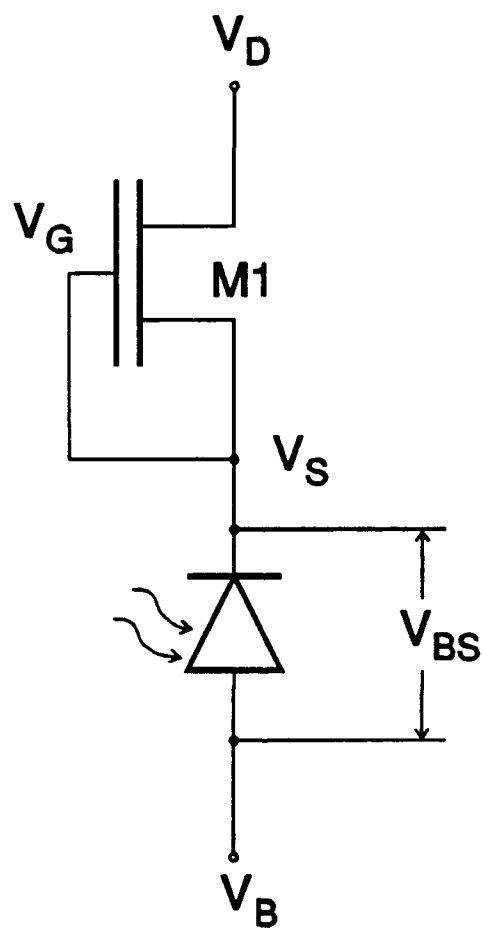


FIGURE 1: LARGE DYNAMIC RANGE PHOTODETECTOR CIRCUIT



drain current achievable is desirable [2]. Another application is found in analog neural networks which exploit the exponential relationship between gate-source bias and drain current [3]. However, most published analysis of the temperature dependence of MOSFETs operated in the subthreshold region concerns the design implications for digital VLSI circuits where it is important to ensure that a transistor biased in the OFF condition does not conduct a significant current over the operating temperature range [4].

The wide dynamic range photodetector circuit is analyzed using an expression for the current given in [5],

$$I_s = (W/L) DqN_D L_B (n_i/N_D)^2 \exp(-\beta V_{BS}) \exp(\beta \phi_{sat}) [1 - \exp(-\beta V_{DS})] (2\beta \phi_{sat})^{-\frac{1}{2}} \quad (3)$$

where

L	=	channel length
W	=	channel width
D	=	diffusion constant $(kT/q)\mu$ , where $\mu$ = carrier mobility
$N_D$	=	channel dopant impurity concentration
$n_i$	=	intrinsic carrier concentration $\propto T^{1.5} \exp(-E_g/2kT)$ , where $E_g$ = bandgap potential ( $\sim 1.1$ eV for Silicon)
$\beta$	=	(thermal voltage) $^{-1} = q/kT$
$V_{BS}$	=	source to substrate voltage
$V_{DS}$	=	source to drain voltage
$L_B$	=	extrinsic Debye length $= [\epsilon_s \epsilon_o / \beta q N_D]^{1/2}$
$\epsilon_s$	=	relative permittivity of Silicon = 11.7
$\epsilon_o$	=	permittivity of free space
$\phi_{sat}$	=	band bending potential at the channel - gate dielectric interface for channel pinch off.

Equation (3) can be solved explicitly as a function of the MOSFET terminal potentials since the term  $\beta \phi_{sat}$  is a function of  $V_{BS}$  and of the effective source to gate voltage  $V_{GS}$ . The relationship is

$$\beta \phi_{sat} = \beta V_{GS} + \beta V_{BS} a^2/2 - a(\beta(V_{BS} + V_{GS}) + a^2/4)^{1/2} \quad (4)$$

with the parameter  $a$  given by

$$a = \sqrt{2} (\epsilon_s / \epsilon_{ox}) (t_{ox} / L_B) \quad (5)$$

where

$t_{ox}$  = gate dielectric thickness  
and  $\epsilon_{ox}$  = relative permittivity of the gate dielectric  
(~ 3.7 for  $SiO_2$ ).

Equation (3) can be rewritten to explicitly show the temperature dependence:

$$I_s = GT^{7/2} \frac{\left[ \exp\left\{\left(-E_g/kT\right) + \left(qV_{GS}/kT + \frac{a^2}{2}(T_o) T_o/T\right)\right\} - a(T_o) T_o/T \left(\frac{q}{kT_o} (V_{BS} + V_{GS}) + \frac{a^2(T_o)}{4}\right)^{1/2} \right] (1 - \exp(-qV_{DS}/kT))}{\sqrt{2} \left[ \left(qV_{GS}/kT + qV_{BS}/kT + \frac{a^2}{2}(T_o) (T_o/T)\right) - a(T_o) \frac{T_o}{T} \left(q(V_{GS} + V_{BS})/kT_o + \frac{a^2}{4}(T_o)\right)^{1/2} \right]^{1/2}} \quad (6)$$

where

$$G = \frac{wD}{L} \left[ \frac{k^5 \epsilon_s \epsilon_o}{N_D^3} \right]^{1/2}$$

contains parameters which are relatively insensitive to terminal voltages or temperature and  $a(T_o)$  is the value of  $a$  at a temperature  $T_o$ . Although some parameters such as  $E_g$  and  $D$  are known to be dependent on temperature [6]-[7], the resultant error is not significant over the range of operating temperatures encountered in most practical applications.

For the wide dynamic range photodetector circuit, Equation (6) can be greatly simplified with minimal errors. First, the physical short circuit between the MOSFET gate and source terminals constrains  $V_{GS}$  to be equal to  $-V_{FB}$ .  $V_{FB}$  is the flatband voltage which is necessary to account for surface states, oxide charge and the metal-semiconductor potential  $\phi_{MS}$ . Theoretical estimates of  $V_{FB}$  are very inaccurate, consequently, it is usually determined experimentally [5].

Second, the term  $(1 - \exp(-qV_{DS}/kT))$  in the numerator can be neglected if the circuit is biased for normal operation. Finally, as the gate to source threshold voltage  $V_{TS}$  of the MOSFET must be negative with  $V_{BS} = 0$  for correct circuit operation, it can be shown that the upper limit for the parameter  $a$  is approximately 2.5 for the usual ranges of silicon process parameters [5]. Since  $(qV_{BS}/kT)$  will be much larger than  $a^2$ , the terms in Equation (6) containing  $a^2$  can be neglected with minimal error.

The simplified equation for  $I_s(T, V_{BS})$  is therefore given by

$$I_s(T, V_{BS}) = \frac{GT^{7/2} \exp[-E_g/kT + qV_{GS}/kT - a(T_o)(T_o/T)(q(V_{GS} + V_{BS})/kT_o)^{1/2}]}{\sqrt{2}(qV_{GS}/kT + qV_{BS}/kT - a(T_o)(T_o/T)(q(V_{GS} + V_{BS})/kT_o)^{1/2})^{1/2}} \quad (7)$$

Equation (3) for the MOSFET subthreshold current is derived from a one dimensional model of the MOSFET channel potential. The accuracy of this model is dependent on the channel length; as this is reduced, various additional phenomena degrade the validity of the model. These include the effects of the source and drain potentials on the MOSFET channel potential, transport effects such as carrier velocity saturation, and high electric field effects such as the injection of electrons into the gate oxide and thereby shifting the flatband voltage [5].

The effect of the MOSFET drain potential on the subthreshold current is useful in the photodetector circuit since it permits the DC operating point for  $V_{BS}$  to be modified by varying the drain voltage  $V_D$ . Furthermore, the dependence of the subthreshold current on the source potential  $V_{BS}$  provides additional compression which may be useful in avoiding excessive signal voltage swings for operation over a large dynamic range.

Consequently, the standard implementations of the photodetector circuit use relatively short gate lengths whose nominal values are bracketed in each wafer fabrication run.

Exact analysis of short channel effects requires numerical simulation since the three dimensional geometry of the device and dopant impurity profiles must be considered. However, a two dimensional model is of some use provided its limitations are understood.

A particularly simple relationship between  $V_{DS}$  and the source-drain current of a short channel MOSFET is given in [4], [6]

$$I_s = I_{SL} \exp(qV_{DS}/\delta kT) \quad (8)$$

where  $I_{SL}$  is the source current given by Equation (3) for the long channel MOSFET model and  $\delta$  is a parameter having a weak dependence on  $V_{DS}$  and determined by numerical or empirical means. Note that  $\delta = \infty$  corresponds to the long channel model.

Consequently, Equation (7), the explicit temperature dependent for the subthreshold current  $I_s$  in the photodetector circuit, can be modified to include the short channel effects of the drain and source voltages

$$I_S(T, V_{BS}, \delta) =$$

$$\frac{\left[ GT^{7/2} \exp \left[ -E_g/kT + qV_{GS}/kT + q(V_{DB} - V_{BS})/\delta kT - a(T_o)(T_o/T)(q(V_{GS} + V_{BS})/kT_o)^{1/2} \right] \right]}{\sqrt{2} (qV_{GS}/kT + qV_{BS}/kT - a(T_o)(T_o/T)(q(V_{GS} + V_{BS})/kT_o)^{1/2})^{1/2}}, \quad (9)$$

where  $V_{DB}$  is the MOSFET drain to substrate voltage.

## 2.2 Photodiode Model

Under reverse bias conditions, the photodiode current  $I_0$  consists of a photocurrent  $I_p$  and a dark current  $I_L$ .  $I_p$  is normally proportional to light intensity and is given by

$$I_p = P \lambda n q / hc, \quad (10)$$

where

- $n$  = quantum efficiency
- $P$  = incident illumination power
- $\lambda$  = wavelength of the light
- $h$  = Planck's constant
- $c$  = velocity of light in free space

Previously reported measurements confirm that the photocurrent has a low sensitivity to temperature and bias voltage [7]-[8].

The photodiode dark current  $I_L$  is largely the result of the thermal generation of carriers in the semiconductor. Two components, a generation current produced by the generation of carriers in the reverse biased depletion layer, and a diffusion current caused by the diffusion of carriers generated in the semiconductor bulk to the depletion layer, can be identified. They are given by [8]:

$$I_{gen} = 1/2 q n_i W(V) A / \tau_o, \quad (11)$$

where

- $W(V)$  = depletion layer width proportional to  $V^x$ , where  $V$  is the reverse bias voltage and  $1/3 \leq x \leq 1/2$
- $\tau_o$  = average carrier lifetime

and

$$I_{diff} = qD_n A n_i^2 / N_A L_n + qD_p A n_i^2 / N_D L_p , \quad (12)$$

where

- $D_n$  = diffusion constant for electrons
- $D_p$  = diffusion constant for holes
- $N_A$  = dopant impurity concentration for p-type semiconductor material
- $N_D$  = dopant impurity concentration for n-type semiconductor material
- $L_n$  = diffusion length of electron in p-type semiconductor material
- $L_p$  = diffusion length of holes in n-type semiconductor material.

For a photodiode fabricated as a n+ diffusion on a p-type substrate, the second term in Equation (12) can be neglected.

The temperature dependence of Equations (11) and (12) is largely determined by that of the  $n_i$  and  $n_i^2$  parameters respectively. Consequently, the temperature dependence of the dark current has the form

$$\begin{aligned} I_L(T) &= I_{gen}(T) + I_{diff}(T) \\ &= H_1 \exp(-E_g/2kT) + H_2 \exp(-E_g/kT) \end{aligned} \quad (13)$$

For silicon diodes reverse biased by more than a few volts, the  $I_{gen}$  component is usually dominant at temperatures up to at least 400°K with the exact crossover temperature being a function of bias voltage and the dopant impurity profile [9]-[10].

Additional mechanisms contributing to dark current such as surface states exist, but these can usually be neglected for high quality silicon photodiodes.

### 3.0 ANALYSIS OF CIRCUIT MODEL FOR TEMPERATURE DEPENDENCE

Since the steady state photodiode and MOSFET currents are equal, it is possible to set up the equality

$$(I_p + I_L(T)) = I_s(V_{BS}, T, \delta) . \quad (14)$$

This is a useful relationship for analyzing the circuit operation. Since the circuit is operated so that  $V_{BS}$  has a substantial DC bias or offset relative to both the drain voltage of the MOSFET and the substrate potential, the temperature dependence of  $V_{BS}$  for constant illumination is of critical importance. It determines the need for temperature calibration/compensation techniques and affects the design of the interface electronics which must be able to operate properly over the range of  $V_{BS}$  that can result from the worst case combination of illumination and temperature extremes.

The dependence of  $V_{BS}$  with respect to temperature is found by evaluating the differential

$$\frac{dV_{BS}}{dT} = \frac{\partial V_{BS}}{\partial (I_S(T, V_{BS}, \delta))} \left( \frac{\partial I_L(T)}{\partial T} - \frac{\partial I_S(T, V_{BS}, \delta)}{\partial T} \right) \quad (15)$$

By neglecting the weak temperature dependence of  $G$ , Equation (15) can be evaluated to yield

$$\frac{dV_{BS}}{dT} =$$

$$\left( \left( \frac{1}{(I_p + I_L(T))} \frac{\partial I_L}{\partial T} \right) - \left( \frac{7/2}{T} + \frac{1}{T^2} (E_g/k - qV_{GS}/k - q(V_{DB} - V_{BS})/\delta k + a(T_o) T_o (q(V_{GS} + V_{BS})/kT_o)^{\frac{1}{2}}) \right. \right. \\ \left. \left. \times \frac{-(kT/q) (q(V_{GS} + V_{BS})/kT_o)^{\frac{1}{2}}}{(1/\delta) (q(V_{GS} + V_{BS})/kT_o)^{\frac{1}{2}} + \frac{1}{2} a(T_o)} \right) \right) \quad (16)$$

where

$$\frac{\partial I_L}{\partial T} \frac{kT}{qI_S} = Eg/2qT: (I_L > I_p) \quad (17)$$

$$\frac{\partial I_L}{\partial T} \frac{kT}{qI_S} = 0: (I_L < I_p) \quad (18)$$

From the examination of these results,  $dV_{BS}/dT$  has only a mild dependence on temperature and is virtually constant over restricted temperature ranges. They also indicate that  $dV_{BS}/dT$  decreases with increasing  $I_p$  due to the dependence of  $V_{BS}$  on  $I_p$ , except for very small values of  $I_p$  where  $I_L$  is important.

Another important performance parameter is the logarithmic slope of the response given by

$$S_R = \log_{10} \frac{\partial V_{BS}}{\partial \ln I_p} \quad (19)$$

$S_R$  represents the change in output voltage resulting from a change in  $I_p$  by one decade. It is desirable that  $S_R$  has a low sensitivity to temperature and  $I_p$ , as complex calibration and correction schemes would otherwise be necessary in applications where accurate measurements of illumination intensity are desirable.

Using Equation (9) yields

$$S_R = -2.3 \frac{I_p}{(I_p + I_L(T))} \left( \frac{kT}{q} \right) \left( \frac{(q(V_{GS} + V_{BS})/kT_o)^{\frac{1}{2}}}{(1/\delta)(q(V_{GS} + V_{BS})/kT_o)^{\frac{1}{2}} + \frac{1}{2}a(T_o)} \right) \quad (20)$$

Except for very low values of  $I_p$  where the ratio  $I_L(T)/I_p$  becomes significant, this result has a weak inverse dependence on  $I_p$  since  $V_{BS}$  is a logarithmic function of  $I_p$ . The temperature dependence of  $S_R$  consists of an explicit component linearly proportional to  $T$  and implicit non-linear components resulting from the temperature dependence of  $I_L(T)$  and  $V_{BS}$ .

#### 4.0 EXPERIMENTAL RESULTS

The output voltage from a photodetector structure on the DALSA D4-100 evaluation device was measured for different combinations of illumination intensity and temperature. Illumination was obtained using a HeNe laser having a wavelength of 632.8 nanometers. Uniform illumination over the photodiode and non-critical requirements for its alignment were ensured by the use of a beam expander. An optical attenuator allowed illumination intensity to be varied over a range of 45 dB. The voltage was directly measured by switching on the reset MOSFET and using a low input bias current amplifier ( $i_{bias} \approx 10^{-12}$  A) to

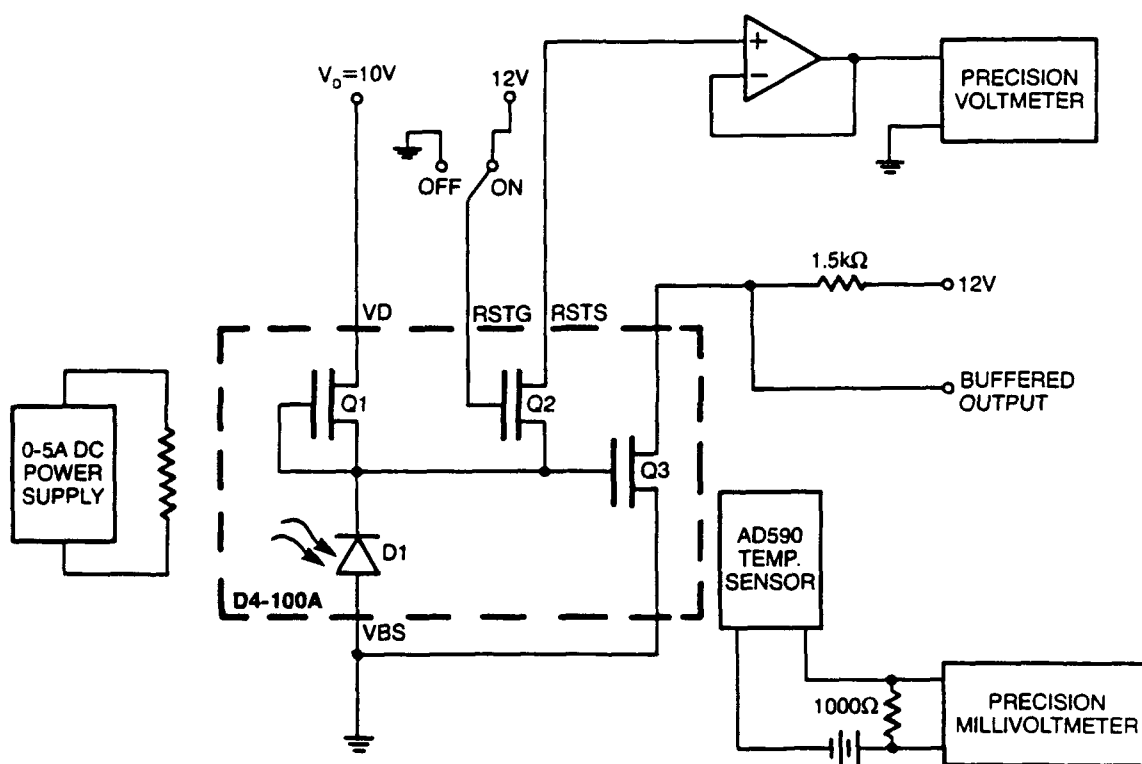


FIGURE 2: EXPERIMENT SET-UP



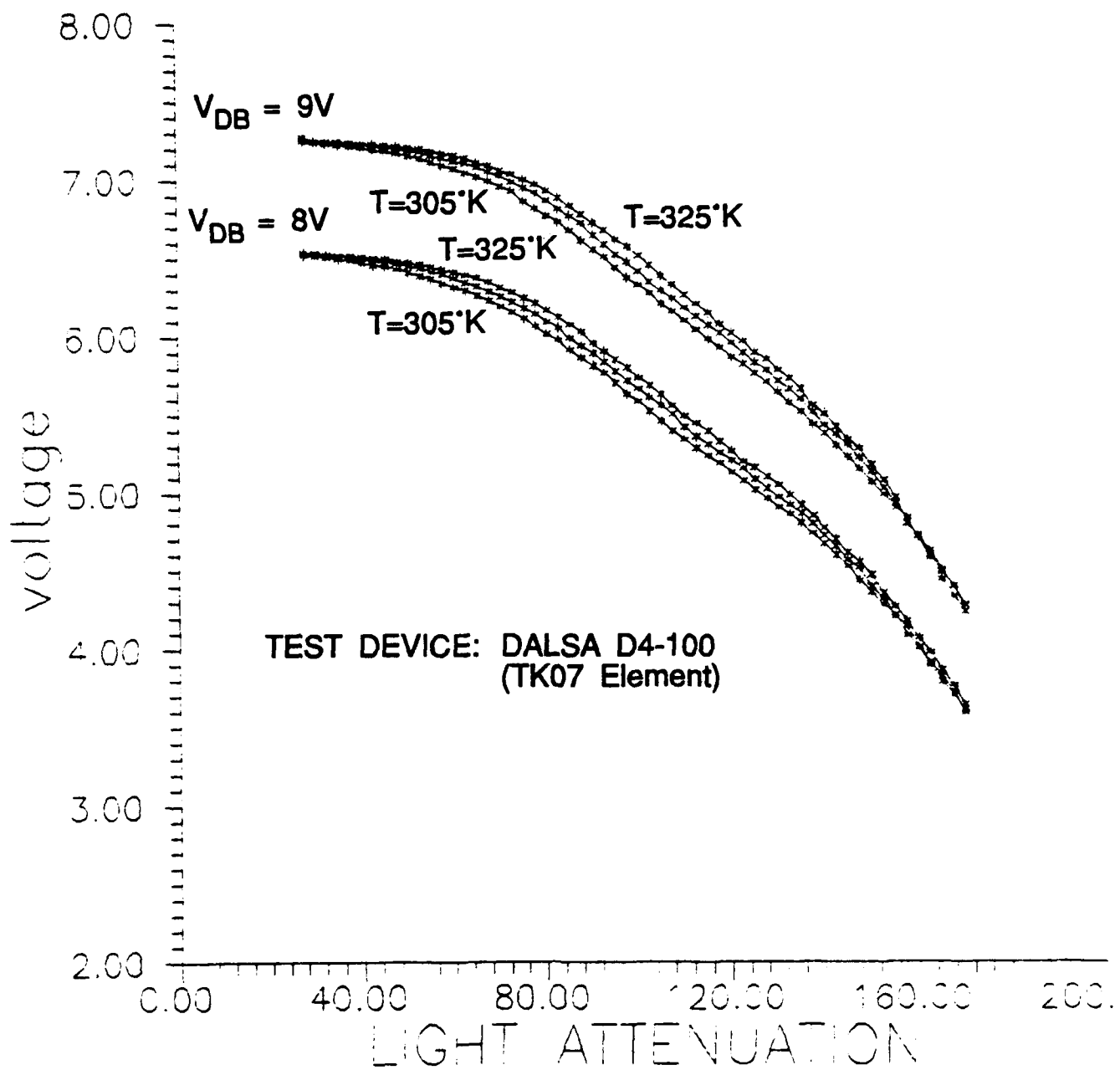


FIGURE 3:  $V_{BS}$  (VOLTS) VS LIGHT ILLUMINATION ATTENUATION  
(INCREMENTS OF 0.3 dB/UNIT)

monitor the voltage at the open circuited reset bias line as shown in Figure 2. Typical results, given in Figure 3, are generally consistent with the analysis.

At 305°K,  $S_R$  and  $dV_{BS}/dT$  are approximately 0.76V/decade and 10 mV/°K over a large range of illumination levels. Using the  $a = 1.74$  determined from the nominal process parameters [13], Equations (20) and (16) can be fitted to the data corresponding to settings of the optical attenuator between 80 and 140 by setting  $V_{GS} = 1.6$  V and  $\delta = 36$  ( $V_{BS} = 6$ V).

At low illumination levels  $S_R$  and  $dV_{BS}/dT$  decrease substantially, as expected from the analysis, but the accuracy of the results is uncertain due to the likelihood that leakage current in the experimental setup is significant.

The dependence of  $V_{BS}$  on  $V_{DB}$  also demonstrates a good fit to the analysis. The 1 volt change in  $V_{DB}$  from 8.0 to 9.0 volts shifts  $V_{BS}$  by approximately 0.7 volts for a wide range of illumination levels. This is reasonable since the substitution of the two sets of values for  $V_{DB}$  and  $V_{BS}$  in Equation (9) results in little change in current.

One area of discrepancy concerns the temperature dependence of  $S_R$  which varies by approximately half the amount predicted by the  $kT/q$  term in Equation (20) for a 20°C temperature change. However, this may be a result of the limitations of the experimental test setup, which did not permit a large temperature range to be used or an accurate direct measurement of the chip temperature of the photodetector device.

## 5.0 DISCUSSION

It is interesting to compare the analytical behaviour of the large dynamic range photodetector circuit with that of a photodiode operated in the solar cell mode. The logarithmic slope of the response of the latter can be derived from Equation (1) as,

$$S_R = 2.3 \frac{mkT}{q} \left( \frac{I_p}{I_p + I_o} \right) . \quad (21)$$

This is similar in form to Equation (20), but differs in magnitude by approximately an order of magnitude due to the difference between  $m$  which is between 1 and 2 and the last term in brackets.

The photodiode output voltage  $V$  has a temperature dependence given by

$$\frac{dV}{dT} = -\frac{1}{T} \left[ (3kT/q + mEg/q) \left( \frac{I_p}{I_p + I_o(T)} \right) - V \right] . \quad (22)$$

Equations (16) and (22) both have a relatively weak ( $\approx 1/T$ ) dependence on temperature and tend to decrease with increasing illumination. The behaviour for the large dynamic range photodetector is more complex in that it is dependent on fabrication process parameters (which affect  $V_{GS}$ ,  $a(T_o)$  and  $\delta$ ), operating conditions ( $V_{DB}$ ) and the MOSFET geometry ( $L$ , dopant profile). If the results of Equations (16) and (22) are normalized with respect to the appropriate  $S_R$ , a useful figure of merit is obtained.

$$F = \left[ \frac{dV}{dT} \frac{1}{S_R} \right]^{-1} . \quad (23)$$

$F$  can be regarded as the temperature change corresponding to an output voltage change that would indicate a change in current by an order of magnitude. For the large dynamic range photodetector, this can be evaluated to yield

$$F = \frac{2.3 I_p}{I_p + I_L(T)}$$

$$\left[ \left( 7/2 + \frac{1}{T^2} (E_g/k - qV_{GS}/k - q(V_{DB} - V_{BS})/\delta k - a(T_o) T_o (q(V_{GS} + V_{BS})/kT_o)^{\frac{1}{2}}) \right) \right] \quad (24)$$

$$\left[ - \frac{1}{(I_p + I_L(T))} \frac{\partial I_L}{\partial T} \right]^{-1} .$$

Similarly, for the photodiode operated in the solar cell mode

$$F = \frac{2.3 I_p}{I_p + I_o(T)} \frac{mkT^2}{q} \left[ (3kT/q + mEg/q) \frac{I_p}{I_p + I_o(T)} - V \right]^{-1} . \quad (25)$$

For operation at 300°K with moderate illumination, typical values of  $F$  would be approximately 68°K and 33°K for Equations (24) and (25) respectively.

A more complete treatment of the problem would involve the generation of a model for  $\delta$  which would include its voltage dependence, the collection of data from a larger number of sample devices whose process parameters have been independently evaluated and a more accurate test setup as proposed in Appendix 1.

## 6.0 REFERENCES

- [1] S.G. Chamberlain and J.P.Y. Lee, "A Novel Wide Dynamic Range Silicon Photodetector and Linear Imaging Array", IEEE Trans. Electron Devices, Vol. ED-31, No. 2, February 1984.
- [2] E. Vittoz and J. Fellrath, "CMOS Analog Integrated Circuits Based on Weak Inversion Operation", IEEE Journal of Solid State Circuits, Vol. SC-12, No. 3, June 1977.
- [3] A.G. Androu et al, "Current-Mode Subthreshold MOS Circuits for Analog VLSI Neural Systems", IEEE Trans. on Neural Networks, Vol. 2, Mar. 1991.
- [4] R.R. Troutman, "Subthreshold Design Considerations for Insulated Gate Field Effect Transistors", IEEE Journal of Solid State Circuits, Vol. SC-19, No. 02, April 1974.
- [5] J.R. Brews, "Physics of the MOS Transistor", Applied Solid State Science, Silicon Integrated Circuits, Part A, Academic Press, 1981.
- [6] R.R. Troutman and S.N. Chakravarti, "Subthreshold Characteristics of Insulated Gate Filed Effect Transistors", IEEE Transactions on Circuit Theory, Vol. CT-20, No. 6, November 1973.
- [7] W. Bludau et al, "Temperature Dependence of the Bandgap of Silicon", Journal of Applied Physics, Vol. 45, pg. 1846, 1974.
- [8] L. Vadasz and A.S. Grove, "Temperature Dependence of MOS Transistor Characteristics Below Saturation", IEEE Trans. on Electron Devices, Vol. ED-13, No. 12, December 1966.
- [9] M.D. Jack and R.H. Dyck, "Charge-Transfer Efficiency in a Buried-Channel Charge Coupled Device at Very Low Signal Levels", IEEE Journal of Solid State Circuits, Vol SC-11, No. 1, February 1976.
- [10] R. Kohler et al, "Temperature Dependent Nonlinearity Effects of a QED-200 Detector in the Visible", Applied Optics, Vol. 29, No. 28, October 1990.
- [11] A.S. Grove, "Physics and Technology of Semiconductor Devices:", Wiley, 1967.
- [12] S. Cheng and P. Manos, "Effects of Operating Temperature on Electrical Parameters in an Analog Process", IEEE Circuits and Devices Magazine, 1989.
- [13] W. Washkurak, private communication.

## APPENDIX 1

### IMPROVED TEST CIRCUIT FOR DC CHARACTERIZATION OF THE DYNAMIC RANGE PHOTODETECTOR CIRCUIT

The test circuit used in the work described in this report has several deficiencies which result from the constraint of having to use a standard production photodetector device. Usually the photodetector circuit is interfaced to an amplifier which is typically a MOSFET operated as either a common source or common drain amplifier or is multiplexed via a CCD Parallel-Input-Serial-Output shift register. However, it becomes difficult to determine what the actual voltage  $V_{gs}$  in the photodetector circuit is since the amplifier transfer function will not be accurately known. Consequently, the direct measurement of the DC voltage from the photodetector must be done via the reset bias voltage input with the reset transistor tuned on. This has the fundamental disadvantage that loading effects will be introduced at low illumination levels. Even if a low input bias current amplifier is used to buffer the signal, as was done for the experimental work described in the report, significant leakage currents can result from contamination of the interconnection between the photodetector and amplifier.

An attractive solution is shown in Figure A-1. This involves the use of a special test device with a pair of matching common drain amplifiers A1 and A2. Amplifier A1 buffers the photodetector voltage and amplifier A2 is used inside the feedback loop of an operational amplifier A3 to compensate for the input to output offset voltage and non-ideal transfer function of amplifier A1. Since the input of amplifier A1 needs not be accessible externally, it has no need for electrostatic protection circuitry which will introduce leakage currents. Consequently, the photodetector circuit operates with negligible DC loading and high accuracy should be achievable.

The test device could also have additional test structures to allow the accurate measurements of the fabrication process parameters.

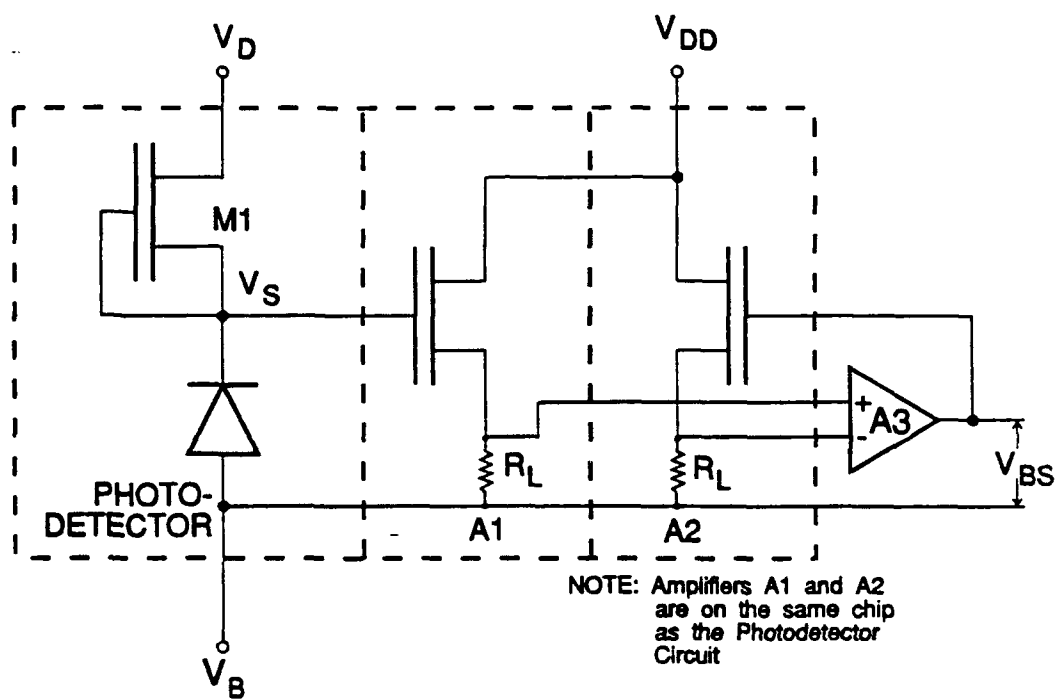


FIGURE A1: IMPROVED PHOTODETECTOR TEST  
CIRCUIT FOR DC CHARACTERIZATION

## DOCUMENT CONTROL DATA

(Security classification of title, body of abstract and indexing annotation must be entered when the overall document is classified)

1. ORIGINATOR (the name and address of the organization preparing the document. Organizations for whom the document was prepared, e.g. Establishment sponsoring a contractor's report, or tasking agency, are entered in section 8.) DEPARTMENT OF NATIONAL DEFENCE DEFENCE RESEARCH ESTABLISHMENT OTTAWA OTTAWA, ONTARIO K1A 0K2		2. SECURITY CLASSIFICATION (overall security classification of the document including special warning terms if applicable)  UNCLASSIFIED	
3. TITLE (the complete document title as indicated on the title page. Its classification should be indicated by the appropriate abbreviation (S.C or U) in parentheses after the title.)  THE TEMPERATURE DEPENDENCE OF A LARGE DYNAMIC RANGE PHOTODETECTOR STRUCTURE (U)			
4. AUTHORS (Last name, first name, middle initial)  INKOL, ROBERT J.			
5. DATE OF PUBLICATION (month and year of publication of document)  DECEMBER 1991	6a. NO. OF PAGES (total containing information. Include Annexes, Appendices, etc.)  22	6b. NO. OF REFS (total cited in document)  13	
7. DESCRIPTIVE NOTES (the category of the document, e.g. technical report, technical note or memorandum. If appropriate, enter the type of report, e.g. interim, progress, summary, annual or final. Give the inclusive dates when a specific reporting period is covered.)  TECHNICAL NOTE			
8. SPONSORING ACTIVITY (the name of the department project office or laboratory sponsoring the research and development. Include the address.)  DEPARTMENT OF NATIONAL DEFENCE DEFENCE RESEARCH ESTABLISHMENT OTTAWA OTTAWA, ONT. K1A 0K2			
9a. PROJECT OR GRANT NO. (if appropriate, the applicable research and development project or grant number under which the document was written. Please specify whether project or grant)  011LB		9b. CONTRACT NO. (if appropriate, the applicable number under which the document was written)	
10a. ORIGINATOR'S DOCUMENT NUMBER (the official document number by which the document is identified by the originating activity. This number must be unique to this document.)  DREO TECHNICAL NOTE 93-35		10b. OTHER DOCUMENT NOS. (Any other numbers which may be assigned this document either by the originator or by the sponsor)	
11. DOCUMENT AVAILABILITY (any limitations on further dissemination of the document, other than those imposed by security classification)  <input checked="" type="checkbox"/> Unlimited distribution <input type="checkbox"/> Distribution limited to defence departments and defence contractors; further distribution only as approved <input type="checkbox"/> Distribution limited to defence departments and Canadian defence contractors; further distribution only as approved <input type="checkbox"/> Distribution limited to government departments and agencies; further distribution only as approved <input type="checkbox"/> Distribution limited to defence departments; further distribution only as approved <input type="checkbox"/> Other (please specify):			
12. DOCUMENT ANNOUNCEMENT (any limitation to the bibliographic announcement of this document. This will normally correspond to the Document Availability (11). However, where further distribution (beyond the audience specified in 11) is possible, a wider announcement audience may be selected.)			



UNCLASSIFIED

SECURITY CLASSIFICATION OF FORM

- 13 ABSTRACT (a brief and factual summary of the document. It may also appear elsewhere in the body of the document itself. It is highly desirable that the abstract of classified documents be unclassified. Each paragraph of the abstract shall begin with an indication of the security classification of the information in the paragraph (unless the document itself is unclassified) represented as (S), (C), or (U). It is not necessary to include here abstracts in both official languages unless the text is bilingual).

(U) A recently developed photodetector circuit exploits the exponential voltage-to-current characteristic of a MOSFET operated in the subthreshold region to achieve a logarithmic steady state response. This paper analyzes the temperature dependence of the circuit operation and presents experimental results demonstrating the capabilities and limitations of the model.

- 14 KEYWORDS, DESCRIPTORS or IDENTIFIERS (technically meaningful terms or short phrases that characterize a document and could be helpful in cataloguing the document. They should be selected so that no security classification is required. Identifiers, such as equipment model designation, trade name, military project code name, geographic location may also be included. If possible keywords should be selected from a published thesaurus, e.g. Thesaurus of Engineering and Scientific Terms (TEST) and that thesaurus-identified. If it is not possible to select indexing terms which are Unclassified, the classification of each should be indicated as with the title.)

PHOTODIODE  
TEMPERATURE DEPENDENCE  
PHOTOCURRENT  
SUBTHRESHOLD EFFECT  
OPERATIONAL AMPLIFIER

UNCLASSIFIED

SECURITY CLASSIFICATION OF FORM